TB43

19th International Symposium of Ballistics, 7–11 May 2001, Interlaken, Switzerland

NUMERICAL FRAGMENTATION MODELING AND COMPARISONS TO EXPERIMENTAL DATA

E. S. Hertel, Jr. and M. E. Kipp

Sandia National Laboratories, Albuquerque, NM, 87185, USA

Previous experiments of a tungsten sphere impacting a thin target indicated that beyond some threshold velocity, the sphere breaks into progressively finer fragments with increasing impact velocity. Timed radiographs have imaged this breakup, and been utilized to determine debris cloud expansion velocities. Numerical simulations of such an impact event clearly demonstrate that the average strain rate calculated from this expansion velocity is not representative of the impact-induced strain rates that produce the fragmentation. Consequently, the average fragment sizes obtained in these experiments must be correlated to strain rates extracted from shock wave code simulations to gain the full benefit of the experiments. An Eulerian shock wave propagation code, CTH, with a fragmentation model has been used to explore the details of these impact scenarios and effectiveness of the methods employed to model the fracture and fragmentation processes.

INTRODUCTION

The prediction of failure and fragmentation in shock physics analysis codes or hydrocodes as they are normally called has been a goal of research activities in the United States and other countries for many years. Staff at Sandia National Laboratories have been actively pursuing rescarch in the statistical aspects of fragmentation along with the implementation of fracture models into hydrocodes, principally through the fragmentation models based on the work of Grady [1]. Kipp, et al. [2,3] implemented early versions of this model into hydrocodes. Concepts to extend the basic average fragment size to a statistical representation were discussed by Kipp, at al. [3]. To accommodate both high strain rate fracture at spall (high-confinement, small strains) conditions and low strain rate fracture (unconfined expansion, large strain to failure), the model described by Johnson and Cook [4] has also been employed. Previous fracture and fragmentation modeling work on tungsten carbide has been reported by Hertel and Grady [5].

Previous numerical analyses of fragmenting cylinders, expanding under explosive loading, have shown excollent agreement with data (Wilson, et al. [6]). In those experi-

ments, the strain rates were relatively uniform throughout the cylinder, and the experimental fragment size data were used to estimate a dynamic fragmentation constant. When estimates of this same parameter were made for the same material under different loading conditions – sphere impact onto thin targets – the estimated strain rate and measured fragment dimensions led to a substantially different coefficient [7]. Numerical results discussed here will show for the current model that these discrepancies can be reconciled when particular attention is paid to the details of the strain rates internal to the sphere.

In the present study, the sphere impact is used to exemplify the fracture and fragmentation modeling progress. Both two- and three-dimensional numerical simulations of the experiments have been made of this impact geometry using the multi-dimensional Eulerian shock physics code, CTH [8].

NUMERICAL IMPLEMENTATION OF FRACTURE

The remarks contained here will focus on Eulerian formulations for the solution of the governing equations. The equations that represent the conservation of mass, momentum, and energy are typically solved in one of two ways, Eulerian or Lagrangian. The Eulerian technique assumes a mesh that is fixed in space and the problem fluid (or material) moves through the mesh as a function of time. The Lagrangian technique assumes a mesh that is fixed with respect to the material and the mesh moves as a function of time.

Both methods have strengths and weaknesses depending on the specific code. Several general comments can be made for the major classes of codes. The Eulerian techniques have several strengths, one of the most important being that they have a simple mechanism for creating free surface in fracture and fragmentation. They are also computationally robust for large deformation material mechanics, and they have simple schemes for mesh development and material insertion. They are, however, usually computationally intensive in run time and memory requirements, have difficulties with surface recognition or material interfaces (Eulerian codes do not explicitly track a surface), and poor numerical techniques can lead to excessive shock diffusion.

Lagrangian techniques solve the conservation equations on a mesh that moves with the material. The conservation equations are generally solved using finite difference or finite element techniques, with finite element techniques being the most popular. Straightforward Lagrangian techniques have several strengths: they can be computationally less intensive in run time and memory requirements and they can accurately recognize material interfaces or surfaces. However, free surface creation to accommodate fracture and fragmentation is difficult and typically relies on ad hoc algorithms, large deformations frequently lead to mesh tangling or inversion, mesh development can be extremely difficult in three-dimensions and may be the limiting factor in very large scale computing problems, and contact surface and slide surface algorithms can be difficult to implement in two-dimensions and three-dimensions.

The Eulerian code, CTH, utilized in the current study is a multi-dimensional, multi-material shock physics analysis package. CTH uses a finite volume scheme to solve the conservation equations of mass, momentum, and energy in a spatially fixed frame of reference. Even though we refer to CTH as an Eulerian code, in reality a two-step solution al-

gorithm is used. The first step is Lagrangian in nature in which the material state is advanced in time, the computational mesh is allowed to distort, and no material crosses cell boundaries. During the second step, the distorted mesh is remapped back to the original mesh and material is fluxed from the old (distorted) cell to the new (original) cell. The remap algorithms are second-order to minimize numerical distortion. CTH is widely used by the United States Department of Defense and Department of Energy Laboratories and their contractors. Typical simulations include shock propagation, penetration and perforation of armor, warhead mechanics, and high explosive initiation and detonation.

The following discussion is specific to CTH but representative of all Eulerian hydrocodes. CTH maintains all internal data at cell centers with the exception of the velocities. Typical cell centered information contained within the CTH database includes material state, such as mass, volume, pressure, energy, stress, and internal state variables. The cell data are known at integral time steps. The velocity data are given at the center of a cell face and is known at half time steps. The staggered mesh (both spatial and temporal) for material state data and velocities allows for a simple calculation of gradients (again, spatial and temporal) and does not require the solution of an elliptic partial differential equation. The reader should note that no information about material interfaces is stored explicitly in an Eulerian code.

Hydrodynamic fracture or spall is modeled by a technique known as “void insertion” where the void material is inserted into a computational cell when that cell exceeds a fracture criteria. At least two known difficulties exist with this technique: one is that although directional information can be used to make a determination the effect of the void insertion is isotropic; two is that a “fractured” region can heal if that region experiences compression. The latter difficulty can be remedied by the use of a scalar damage model where an internal state variable tracks material failure and memory of the failure is advected with the material motion [4]. In CTH, the scalar damage models are coupled to the tensile stress (σf) criteria by the following:

$$\sigma_f = \sigma_s + (v_t - \sigma_s)\, D, \tag{1}$$

so that the initial fracture stress is the spall stress (σ_s) when damage (D) is zero, but continuously evolves to the quasi-static fracture stress (σ_t) as the damage approaches unity. The damage (D) is based on the Johnson-Cook fracture scheme, an integral of the equivalent plastic strain [4]. Since this and other similar models affect the local stress-state, they are coupled to the continuum mechanics and affect material motion. The statistical fragmentation models of Grady and Kipp [1–3] as currently implemented into CTH are not coupled to the continuum mechanics and do not affect material motion. Past use of the statistical fragmentation model did not track the fragment distribution until the material was fully damaged (D=1). This led to a significant under prediction of the fragmented mass [2] for the sphere impact. Experimentally, both geometries – sphere impact and the explosively loaded cylinder – effectively undergo complete fragmentation. The use of both models has led to some inconsistencies between the continuum predictions and the statistical description of fragmentation. The remainder of this paper will describe some of the inconsistencies and their resolution.

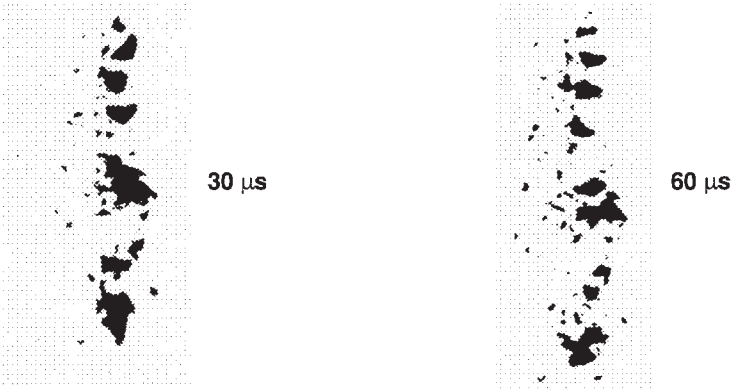

Figure 1. Radiographic images of tungsten debris at approximately 30 and 60 μs after tungsten sphere (0.25" diameter, 2550 m/s) impact onto a thin target Lucalox plate (from Grady, et al. [7]).

EXPERIMENTAL OBSERVATIONS

The impact of a sphere with a thin target plate results in an expanding debris cloud of fragmented sphere material. Fig. 1 shows two sequential radiographs at 30 and 60 μs after impact of a tungsten sphere (0.25" diameter, 2550 m/s) with a Lucalox target (0.10" thick) [7]. The axial width of the debris is comparable to the original diameter of the sphere, and the diameter of the debris cloud is expanding at an acquired velocity that depends on the impact velocity.

NUMERICAL MODEL AND SIMULATIONS

Numerical analysis of this tungsten sphere impact was made with the multi-dimensional Eulerian shock physics code, CTH. In order to accommodate the impact and expansion of the sphere in three dimensions, the impact was simulated in a physical space of 3 cm x 3 cm x 1.7 cm. This region was uniformly resolved with 0.1 mm cubical cells. Typical calculations utilized about 15 million cells. The tungsten was modeled as a Mie-Gruniesen solid, with constant yield strength of 1.4 GPa, Poisson ratio of 0.279, and a fracture strength that varied from its spall stress at high strain rates (2.0 GPa) to a uniaxial tensile stress (0.9 GPa) at low strain rates and large strain (30%). Properties of the tungsten include a density of 17.60 g/cm^3, bulk sound velocity of 4030 m/s, linear U_s–U_p coefficient of 1.237, and a fracture toughness of 30 MPa-m$^{1/2}$. The Lucalox plate was simulated using the Johnson-Holmquist [9] ceramic model for Al_2O_3.

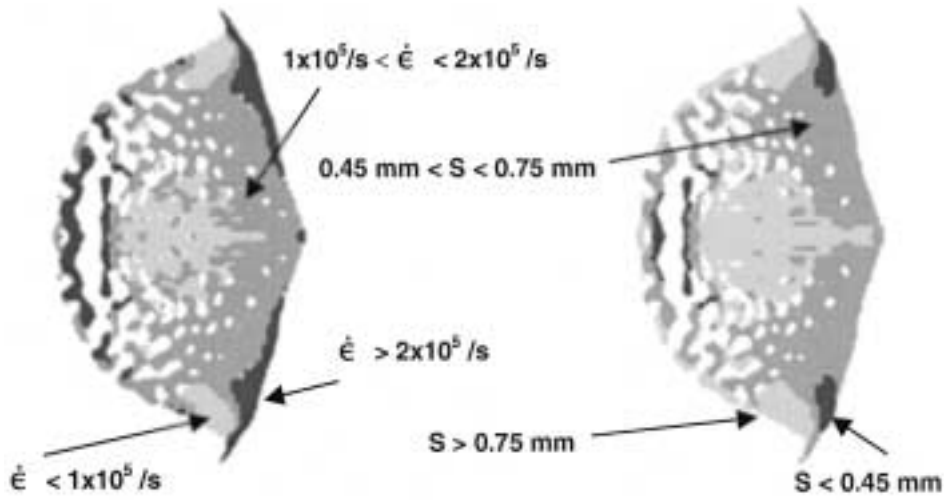

Figure 2. Tungsten sphere at 5 μs after impact with a thin target Lucalox plate, from two-dimensional numerical simulation. Left: strain rate ($\dot{\varepsilon}$) regions; Right: average fragment size (S) regions.

DISCUSSION OF EXPERIMENTAL AND NUMERICAL RESULTS

The state of the tungsten sphere at 5 μs is illustrated in Fig. 2 for a two-dimensional axisymmetric impact simulation. Two images are included that provide insight into the fracture strain rate and average fragment sizes. Both the strain rate and fragment sizes are partitioned into three regions each: strain rate ranges of 0–$1x10^5$/s, $1x10^5$–$2x10^5$/s, and >$2x10^5$/s; and average fragment size ranges from 0–0.45 mm, 0.45–0.75 mm, and >0.75 mm. Generally, regions of small fragments are associated with high strain rates and visa versa [1].

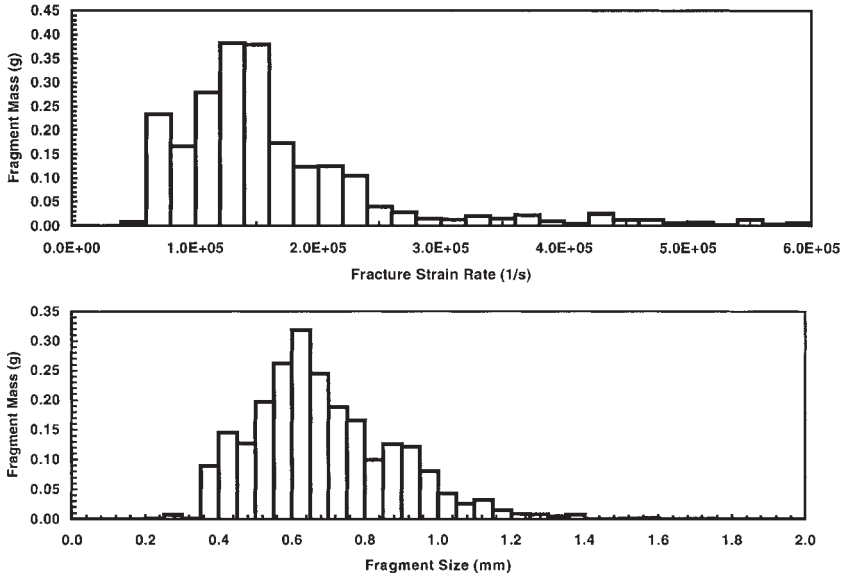

Figure 3. Histograms from two-dimensional numerical simulation of the tungsten debris at 5 μs after tungsten sphere impact onto a thin target Lucalox plate. Bottom: distribution of total fragment mass vs. average fragment size; Top: distribution of fragment mass vs. strain rate at the time of

Histograms from a two-dimensional simulation of the tungsten response to the impact are included in Fig. 3. Approximately 99% of the initial 2.36 g sphere mass has fragmented. Pragmentation of the sphere is complete by 3 μs after impact, by which time the distribution is quite stable. The fragment size and strain rate distribution plots in Fig. 3 are taken at 5 μs after impact. The mean mass of fragments is at a characteristic fragment dimension of about 0.6 mm (Fig. 3, bottom), which is in excellent agreement with the size estimated from the experimental radiographs [7]. However, the average strain rate reported in [7] (3.8×10^4/s) is considerably smaller than the dominant strain rate obtained from the simulations (~1.4×10^5/s), as is clear from the histogram in Fig. 3 (top). The primary reason for the difference is that the strain rate calculated from the induced expansion velocity in the experimental analysis is not representative of the strain rates experienced by the sphere that lead to fracture and fragmentation. Explicitly, the larger strain rates obtained numerically are controlling the fragmentation, and the induced expansion velocity of the debris is a consequence of the fragmentation, not a contribution to the process. Using the same fragmentation parameters in the simulations of both this impact event and the previously reported cylinder test results [6] lead to average fragment size results that are consistent with both experimental measurements.

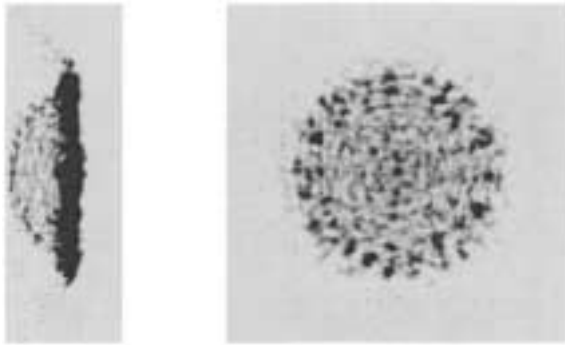

Figure 4. Synthetic radiographs of tungsten sphere at 30 μs after impact with a thin target Lucalox plate, from three-dimensional numerical simulation. Left: view normal to axis of impact; Right: view parallel to axis of impact.

The calculated decrease in axial velocity is about 190 m/s, compared to an experimental value of 220 m/s. These simulations of the impact event result in expansion velocities that are higher than those measured – in this impact simulation the expansion velocity is about 200 m/s compared to the measured one of 99 m/s [7].

When a three-dimensional simulation of this sphere impact event is extended to the time of the frst experimental radiograph (~30 μs), the breakup and expansion of the tungsten can begin to be observed numerically. Synthetic radiographs from the simulation are shown in Fig. 4. On the left is the same view as that of the experiment (Fig. 1) and on the right is a view along the axis of impact. The latter view clearly illustrates the breakup of the tungsten by this time (although the "fragments" on these radiographs are a consequence of local code factors and not defined or constrained by the uncoupled fragmentation model).

CONCLUSIONS

Consistent fragment characteristics from two distinctly different geometries – explosively loaded cylinders and sphere impacts – can be calculated with the same material parameters. In the original implementation of the Grady-Kipp model, the statistical representation was not initiated until the material underwent complete damage (D=1). When the implementation was modified to allow the fragment statistics to be calculated for any damage level, the comparison of data to simulation improved significantly. Key to this result is the observation that in the sphere configuration, the strain rates during the fracture process are much larger than the inferred average strain rates derived from the late time debris expansion velocity. Fracture models that accumulate a wide range of loading conditions are required to address these diverse geometries. In the cylinder test configuration, the large expansion strain to failure occurs at relatively small strain rates over a long period of time; stress wave interactions within the impacted sphere occur at very large strain rates over very short periods of time.

ACKNOWLEDGEMENTS

Sandia is a multi-program laboratory operated by Sandia Corporation, a Lockhoed Martin Company, for the United States Department of Energy under Contract DE-AC04-94AL85000. Funding was provided in part under the United States Department of Defense/Department of Energy Office of Munitions Memorandum of Understanding. The authors gratefully acknowledge the radiographs provided by D. E. Grady, ARA, Albuquerque, NM, USA, shown in Fig. 1.

REFERENCES

1. D. E. Grady, "The Spall Strength of Condensed Matter," J. Mech. Phys. Solids, 36, 353–384, 1998
2. M. E. Kipp, D. E. Grady, and J. W. Swegle, "Numerical and Experimental Studies of High-Velocity Impact Fragmentation," Int. J. Impact Engng, 14, 427–438, 1993
3. M. E. Kipp, D. E. Grady, and J. W. Swegle, "Experimental and Numerical Studies of High-Velocity Impact Fragmentation," Sandia National Laboratories Report SAND93-0773, 1993
4. G. R. Johnson and W. H. Cook, "Fracture Characteristics of Three Metals Subjected to Various Strains, Strain Rates, Temperatures, and Pressures" J. Engng. Frac. Mech., 21, 31–48, 1985
5. E. S. Hertel and D. E. Grady, "Tungsten Carbide Fragmentation: Experimental Characterization and Numerical Modeling," in the Proceedings of the 15th International Symposium on Ballistics, Jerusalem, Israel, May 21–24, 1995
6. L. T. Wilson, D. R. Reedal, M. E. Kipp, R. R. Martinez, and D. E. Grady, "Comparisons of Calculated and Experimental Results of Fragmenting Cylinder Experiments," for Explomet 2000, Fundamental Issues and Applications of Shock-Wave and High Strain-Rate Phenomena, Albuquerque, NM, June 19–22, 2000
7. D. E. Grady, L. C. Chhabildas, W. Reinhart, D. R. Reedal, and L. T. Wilson, "Impact and Explosion Induced Failure and Fragmentation Studies on Tungsten," Proceedings 15th US Army Symposium on Solid Mechanics, Myrtle Beach, SC, April 12–14, 1999
8. E. S. Hertel, Jr., R. L. Bell, M. G. Elrick, A. V. Farnsworth, G. I. Kerley, J. M. McGlaun, S. V. Petney, S. A. Silling, P. A. Taylor, and L. Yarrington, "CTH: A Software Family for Multi-Dimensional Shock Physics Analysis," Proceedings of the 19th International Symposium on Shock Waves, Volume 1, 377–382, Marseilles, France, July 26–30, 1993
9. G. R. Johnson, T. J. Holmquist, J. Lankford, C. E. Anderson, and J. Walker, "A Computational Constitutive Model and Test Data for Ceramics Subjected to Large Strains, High Strain Rates, and High Pressures," Honeywell Report, DE-AC04-87AL-42550, 1990